

Document downloaded from the institutional repository of the University of Alcalá: <http://ebuah.uah.es/dspace/>

This is a preprint version of the following published document:

Regadío, A. & Sánchez-Prieto, S. 2018, "Unfolding and unfoldability of digital pulses in the z-domain", Nuclear Instruments and Methods in Physics Research Section A, vol. 888, pp. 228-234

Available at <http://dx.doi.org/10.1016/j.nima.2018.01.089>

© 2018 Elsevier

(Article begins on next page)



This work is licensed under a

Creative Commons Attribution-NonCommercial-NoDerivatives
4.0 International License.

Unfolding and unfoldability of digital pulses in the z-domain

Alberto Regadío^{a,*}, Sebastián Sánchez-Prieto^b

^a*Electronic Technology Area, Instituto Nacional de Técnica Aeroespacial, 28850 Torrejón de Ardoz, Spain*

^b*Department of Computer Engineering, Space Research Group, Universidad de Alcalá, 28805 Alcalá de Henares, Spain*

Abstract

The unfolding (or deconvolution) technique is used in the development of digital pulse processing systems applied to particle detection. This technique is applied to digital signals obtained by digitization of analog signals that represent the combined response of the particle detectors and the associated signal conditioning electronics. This work describes a technique to determine if the signal is unfoldable. For unfoldable signals the characteristics of the unfolding system (unfolder) are presented. Finally, examples of the method applied to real experimental setup are discussed.

Keywords: Unfolding, Synthesis, Deconvolution, Digital pulse processing, Pulse shaping

1. Introduction

In radiation spectroscopy, the development of Digital Pulse Processing is usually focused on direct synthesis of pulse shapes using digitized signals coming from particle detection used in radiation measurement systems [1, 2]. The ideal shaping for a given detector depends on the shape of the Digital Pulse Processing (DDP) system input signal and the associated noise characteristics [3]. Thus, specific techniques are used to synthesize various shapes to maximize their Signal-to-Noise Ratio [4–6] or to minimize the effect of ballistic deficit or to reduce the pulse pile-up [1].

A subset of Digital Pulse Processing is the unfolding (or deconvolution) technique that allows the transformation of the digitized signal into a unit impulse in the discrete-time domain (see [7] and the references therein). The unfolding technique can be applied to linear pulse processing systems that are either time-invariant or time-variant. A detection system that uses this technique usually includes the unfolding of the digital signals into unit impulses, followed by the synthesis of digital signal processing systems with unit impulse responses equivalent to the desired pulse shape.

In this paper, we describe a technique to determine if a pulse shape can be unfolded (unfoldability), and in such case, a method that allows the synthesis of its unfolders, either exactly or as a close approximation. The proposed method is suitable for real-time implementation.

*Corresponding Author

Email addresses: regadioca@inta.es (Alberto Regadío), sebastian.sanchez@uah.es (Sebastián Sánchez-Prieto)

29 **2. Unfolding and unfoldability**

In general, digital unfolding systems have a unit impulse response $h[n]$ whose convolution with the input signal $x[n]$ produces a unit impulse $\delta[n]$ as explained in [8]

$$x[n] * h[n] = \delta[n - d], \quad d \in \{0, 1, 2, \dots\} \quad (1)$$

30 where d is the delay of the unit impulse in cycles.

Since Eq. (1) is a convolution, in the z -domain, it can be presented as follows

$$X(z) \cdot H(z) = z^{-d} \quad (2)$$

Therefore, the shaper that unfolds the pulse is equal to

$$H(z) = \frac{z^{-d}}{X(z)} \quad (3)$$

31 On the other hand, when the z -transform is applied to $x[n]$, the arrangement of its poles and their zeros
 32 are obtained. It is also known that systems are stable when all its poles are inside the Region Of Convergence
 33 (ROC) (i.e. $z < 1$), oscillating when at least one of its poles is at the circle $z = 1$ and unstable when at
 34 least one of its poles is outside the ROC (i.e. $z > 1$).

35 When $d = 0$, according to (3), $H(z)$ is the inverse of $X(z)$. It implies that the zeros of $X(z)$ are the poles
 36 of $H(z)$ and vice versa. In addition, $H(z)$ must be stable. Therefore, for a signal $X(z)$ to be unfoldable,
 37 both its zeros and poles must be within the ROC (i.e. $z < 1$).

38 When $d > 0$, $X(z)$ is delayed by d cycles, so the result $X(z) * H(z)$ must be a unit impulse delayed
 39 by d cycles (i.e. $z^{-d}\delta(z)$). Adding a delay of a certain number of cycles implies the inclusion of the same
 40 number of poles in $H(z)$ at $z = 0$. These poles have no effect on the stability of $H(z)$ but their inclusion
 41 may be mandatory to convert a non-casual unfolder obtained into a casual one by applying (3). As very
 42 simple example, if $X(z) = \frac{1}{z-0.5}$, its unfolder is $H(z) = z - 0.5$ which is non-casual. To convert $H(z)$ into
 43 casual it must be delayed by one (or more) cycles, that is $H(z) = \frac{z-0.5}{z}$ whose convolution with $X(z)$ gives
 44 a unit impulse delayed one pulse.

45 Eq. (3) has solution only for signals whose poles and zeros are inside the ROC (e.g. exponential and
 46 (RC) ^{n} pulses). In contrast, whenever a shape is symmetric (e.g. trapezoidal, triangular or cusp-like),
 47 their zeros are located at $|z| = 1$. Consequently, its unfolder has their poles located at $|z| = 1$ and the
 48 unfolder is oscillating or potentially unstable. Fortunately, pulses coming from a radiation detector are
 49 rarely symmetric. In Table 1 the characteristics of the unfolder $H(z)$ as function of the input signal $X(z)$
 50 are listed.

51 It is known that convolution in time-domain is equal to multiplication in the z -domain. Thus, when
 52 two signals are convoluted in time-domain it is equivalent to join all their zeros and poles. As mentioned

Unfolder characteristic	Input signal characteristic	Consequence in the unfold
IIR	Zeros at $z \neq 0$	Poles at $z \neq 0$
Oscillating, potentially unstable	\exists zeros at $ z = 1$	\exists poles at $ z = 1$
Unstable	\exists zeros at $ z > 1$	\exists poles at $ z > 1$
Non-causal	Grad num $<$ grad den	$H(z)$: Grad num $>$ grad den

Table 1: Unfolder characteristics. Non-causal unfolders are not implementable, but they can be solved by adding d grades in the denominator and thus shifting by d cycles the unit impulse as explained in text.

53 previously, the placement of their zeros indicate when signals are unfoldable. Therefore, the result of the
54 convolution of two unfoldable signals is also unfoldable. In contrast, the result of the convolution of an
55 unfoldable signal and a non-unfoldable signal is non-unfoldable. By last, the addition of non-unfoldable
56 signals are also non-unfoldable. These facts are always valid unless the two combined signals cancel out each
57 of their zeros reciprocally. In this case, a new analysis have to be carried out.

58 3. Examples

59 3.1. Unfolding of exponential pulses

In the discrete-time domain, a generic exponential pulse can be defined as

$$x[n] = A \cdot \exp\left(\frac{-n}{\tau}\right) \quad (4)$$

where τ is the decay constant. In the z -domain, it becomes

$$X(z) = \frac{z}{z - a} \quad (5)$$

where

$$a = \exp\left(\frac{-\Delta T}{\tau}\right) \quad (6)$$

60 and ΔT is the sample period of the digitized signal.

Applying the exposed method, we obtain the following unfold with no delay (i.e. $d = 0$)

$$H(z) = \frac{z - a}{z} \quad (7)$$

61 The impulse response in time-domain and pole-zero maps of $X(z)$, $H(z)$ and $Y(z)$ are shown in Fig. 1.
62 This result agrees with that shown in [7] for exponential pulses.

63 3.2. Sum of exponential pulses

64 As stated in [7] and according to the explanation given in Section 2, the unfolding of an exponential
65 pulse can be extended to additions of exponential pulses.

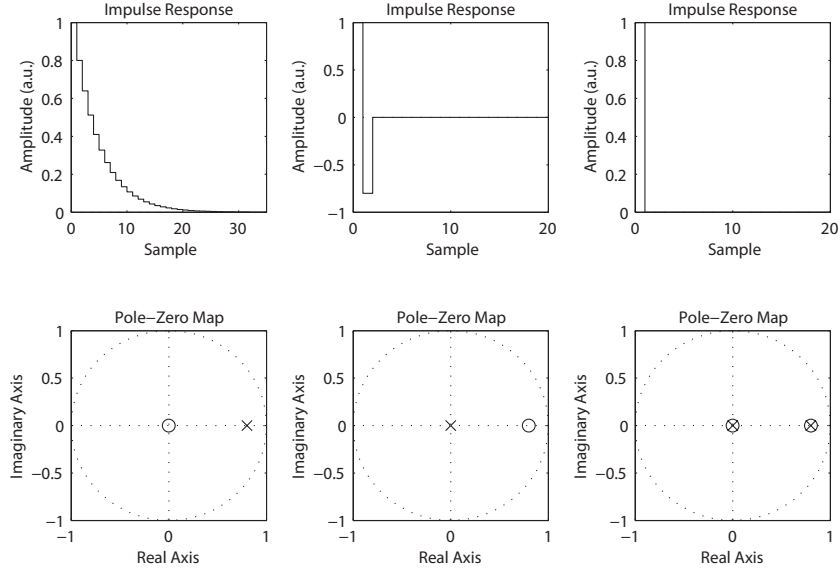


Figure 1: Unfolded exponential signal (right) of an input signal (left) using an exponential unfold (center). In this example, $a = 0.8$.

Using the linearity property of the z-transform, the sum of two exponential pulses can be expressed in the z-domain as

$$X(z) = X_a(z) + X_b(z) = \frac{Az}{z-a} + \frac{Bz}{z-b} \quad (8)$$

where A, B are their amplitudes and a, b are their delay constants. Disregarding A and B , which do not affect the stability of the system, the equation can be rewritten in the following way

$$X(z) = \frac{z((z-a) + (z-b))}{(z-a)(z-b)} \quad (9)$$

66 Recall that for the system to be unfoldable, both poles and zeros must be within the ROC region. Clearly,
 67 the poles of $X(z)$ are the poles of $X_a(z)$ and the poles of $X_b(z)$. All the poles of $X(z)$ will be within the
 68 ROC if those of $X_a(z)$ and $X_b(z)$ are too. With respect to the zeros, the system has one at $z = 0$ and
 69 another at $z = (a+b)/2$, so if $a, b < 1$, the zeros will also be within the ROC.

70 In general, (9) can be extended to an arbitrary number of exponentials and it is trivial to demonstrate
 71 that $X(n)$ is unfoldable whenever their decay constants are below 1. Therefore, we can conclude that the
 72 sum of exponential pulses are unfoldable.

73 In the case where one of the pulses is delayed with respect to the others, this affirmation cannot be
 74 always true since new poles are added and they can make the system unstable or oscillating. In Fig. 2 an
 75 oscillating unfold shaper is shown. The input signal is the sum of two exponential signals with $a = b = 0.8$,
 76 one of them is delayed by one cycle.

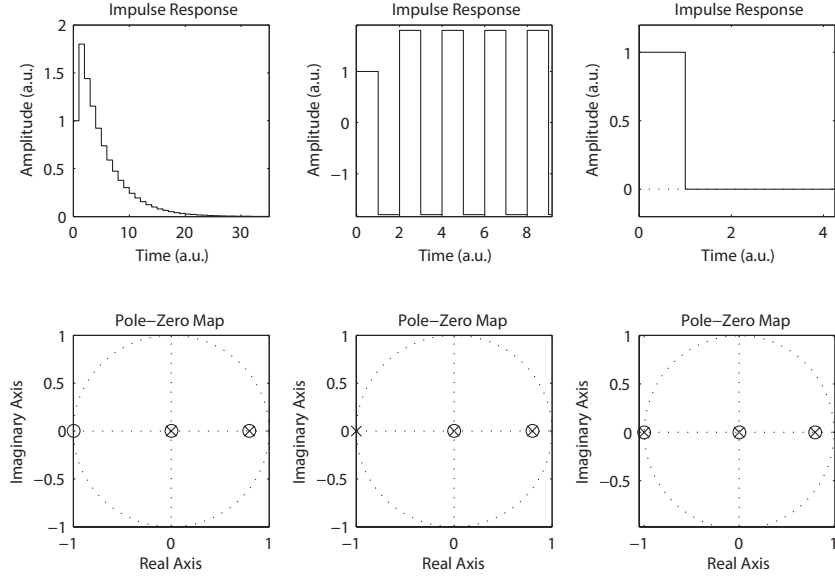


Figure 2: Unfolded signal (right) of a sum of two exponential signals with 2 poles in total (left) using an oscillating unfolders (center).

77 *3.3. Convolution of exponential pulses and $(RC)^n$ pulses*

78 As exposed in Section 2, the convolution of exponential pulses in time-domain is equivalent to multiplication
 79 in z-domain. Thus, the effect of convolving signals is to add new poles and zeros without displacing the
 80 original ones. Therefore, because exponential pulses are unfoldable, the convolution of exponential pulses
 81 are unfoldable.

An arbitrary convolution of exponential pulses gives rise to $(RC)^n$ pulses. This pulse can be represented in the z-domain as

$$X(z) = \frac{z^2}{(z - a)^2} \tag{10}$$

Applying the exposed method, we obtain the following unfolders with no delay (i.e. $d = 0$):

$$H(z) = \frac{(z - a)^2}{z^2} \tag{11}$$

82 The impulse response in time-domain and pole-zero maps of $X(z)$, $H(z)$ and $Y(z)$ are shown in Fig. 3.
 83 This result also agrees with that shown in [7] for exponential pulses.

84 *3.4. Derivatives and integrals of unfoldable signals*

85 It is known that given an input signal $X(z)$, its derivative is $\left(\frac{z-1}{z}\right)^n X(z)$ whereas its integral is $\left(\frac{z}{z-1}\right)^n X(z)$.
 86 In both cases $X(n)$ is multiplied by $\left(\frac{z-1}{z}\right)^n$ ($n = 1$ in case of the derivative $n = -1$ in case of integral).

87 Thus, given a stable signal $X(z)$, $\left(\frac{z-1}{z}\right)^n X(z)$, $n \in \mathbb{Z}$ will be also stable if either poles and zeros of $\left(\frac{z-1}{z}\right)^n$
 88 are within the ROC. In case of integrals ($n \leq -1$), the poles are located in $z = 1$ being able to make the

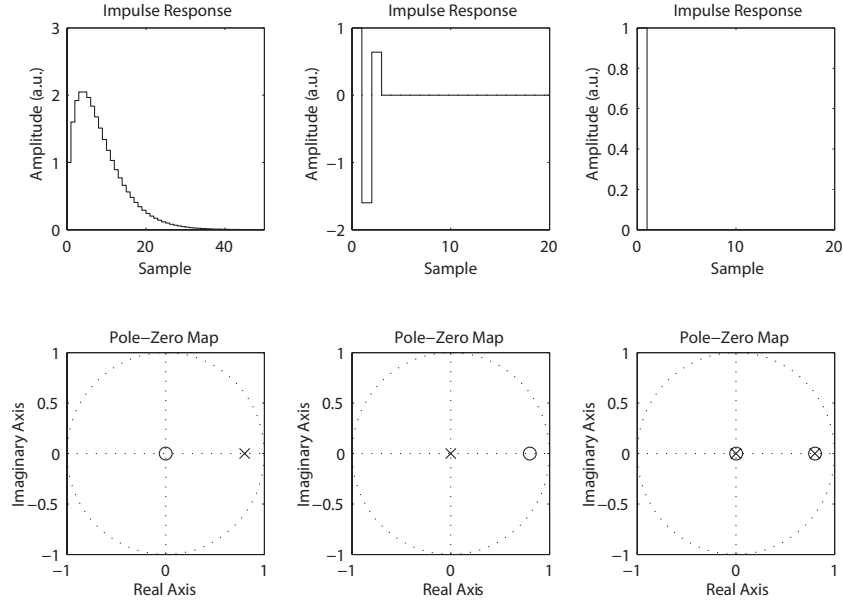


Figure 3: Unfolded signal (right) of an input RC signal (left) using an unfolders (center). The decay constant is $a = 0.8$. Both zeros and poles are of order $m = 2$. Either poles and zeros are double and located at the same place that in Fig. 1.

89 system oscillating or unstable depending on $X(z)$. However, due to the fact that $\left(\frac{z-1}{z}\right)^n$ itself is unfoldable
 90 (see Section 2), we can conclude if a signal is unfoldable, its n-derivative or n-integral is also unfoldable.

91 To illustrate this fact, Fig. 4 and 5 show an example of the derivative and integral of an exponential
 92 signal respectively. The location of the poles and zeros changes depending on whether the signal is derived
 93 or integrated, but the location of the poles and zeros of the exponential (see Fig. 1) does not change.

94 Additionally, applying the properties of the z-transform (decimation, time shifting, etc.), it can be
 95 predicted if a transformation of a pulse are unfoldable from another pulse.

96 4. Input signal modeling

97 To obtain an unfolders as simple as possible it is necessary to correctly model the input signal.

98 In the examples we have just shown, such modeling was trivial: the exponential signal is modeled by
 99 Eq. (5), the step signal is a particular case with $a = 0$ and the unit impulse is another particular case
 100 with $a = \infty$. As we have also shown, $(RC)^n$ signals can be obtained by convolution (multiplication in the
 101 z-domain) of exponential signals.

102 However, for more complex signals, the unfolders may also become more complex. In Fig. 6 can be
 103 observed an example of the unfolding of an exponential signal represented as a sequence of unrelated pulses
 104 ($x[n] = 1 + 0.8z^{-1} + 0.64z^{-2} + \dots$). This signal, despite more complex, is similar than obtained using (5).
 105 Their unfolders response is also similar. It can be observed comparing Fig. 1 with Fig. 6; in both cases
 106 $a = 0.8$.

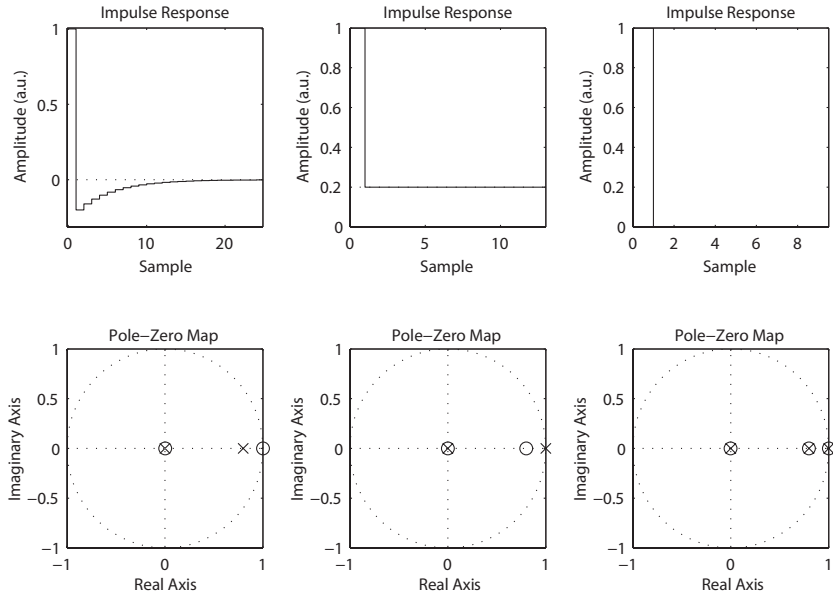


Figure 4: Unfolded signal (right) of a derivative of an exponential pulse (left) using an unfold (center). The exponential pulse has $\alpha = 0.8$.

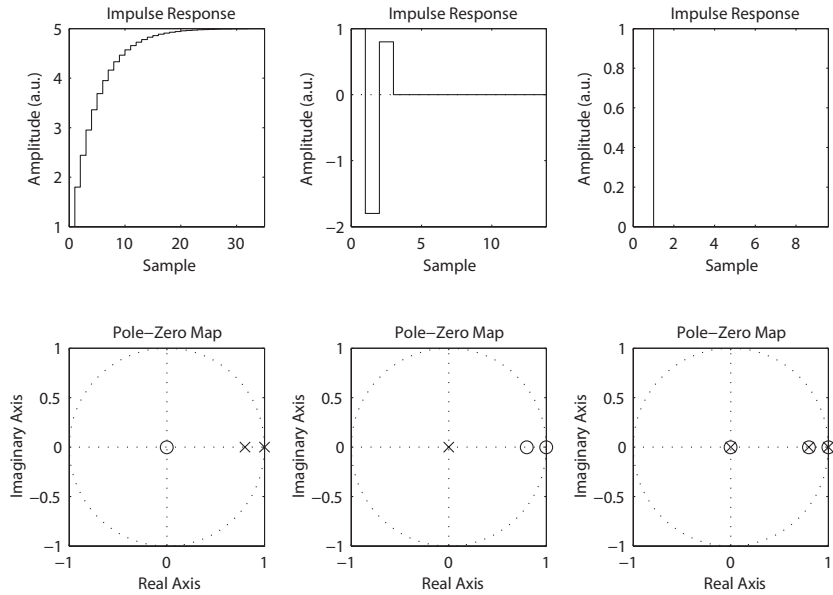


Figure 5: Unfolded signal (right) of an integral of an exponential pulse (left) using an unfold (center). The exponential pulse has $\alpha = 0.8$.

107 The complexity of the unfold is directly proportional to the complexity of the signal. Thus, whether
 108 we want to simplify the unfold, we have to take into account that the signals whose equation is simpler are
 109 those that their current values are related to their previous values. One example is the exponential signal
 110 (see Eq. (5)) but there are many others. This also occurs with Infinite Impulse Response (IIR) filters, which

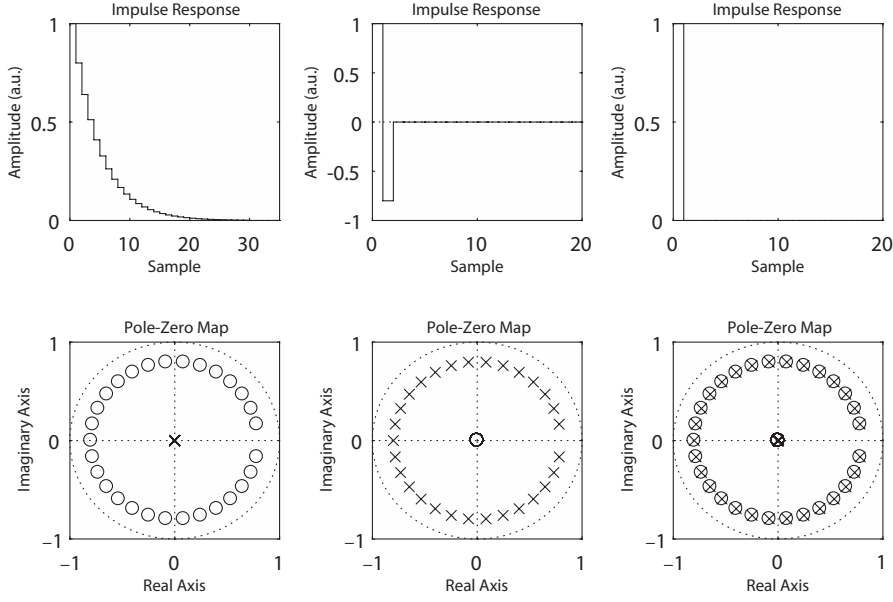


Figure 6: Unfolded exponential signal (right) of an input signal (left) using an unfolders (center). The exponential pulse has been modeled as a FIR pulse of order $N = 20$ coefficients. In this example, $a = 0.8$.

111 usually have a simpler equation than Finite Impulse Response (FIR) filters. Procedures to simplify signals
 112 relating their current values with their previous values can be found in [9, 10].

113 5. Experimental tests

114 The unfolding method presented in this paper has been tested using a signal coming from a radiation
 115 detector. This test has been carried out in the Castilla-La Mancha Neutron Monitor (CaLMA) located in
 116 Guadalajara, Spain. The instrument was made up of fifteen proportional gas counter tubes. In this test,
 117 a tube LND2061 connected to a Canberra ACHNA98 preamplifier was used. More information about the
 118 characteristics, setup and results of this facility can be found in [11].

119 The signal from the preamplifier was digitized by an ADC with sampling period $T_s = 1 \mu s$. The signal
 120 from the ADC is shown in the top graphs of Fig. 7. The signal shown in the bottom graph of both figures
 121 is the result of unfolding the pulses according to the explained method.

The input signal was modeled as a system of 21th order whose transfer function is

$$h_i(z) = x_1 + x_2 z^{-1} + x_3 z^{-2} + \dots + x_{21} z^{-20} \quad (12)$$

122 Thereby, this pulse has a pole at $z = 0$ of order $k = 20$.

123 The output signal (ideally a unit impulse) was delayed by one cycle ($d = 1$). According to (3), the
 124 unfolders has been modeled as $h(z) = \frac{z}{h_i(z)}$. The input signal model, impulse response of the unfolders and

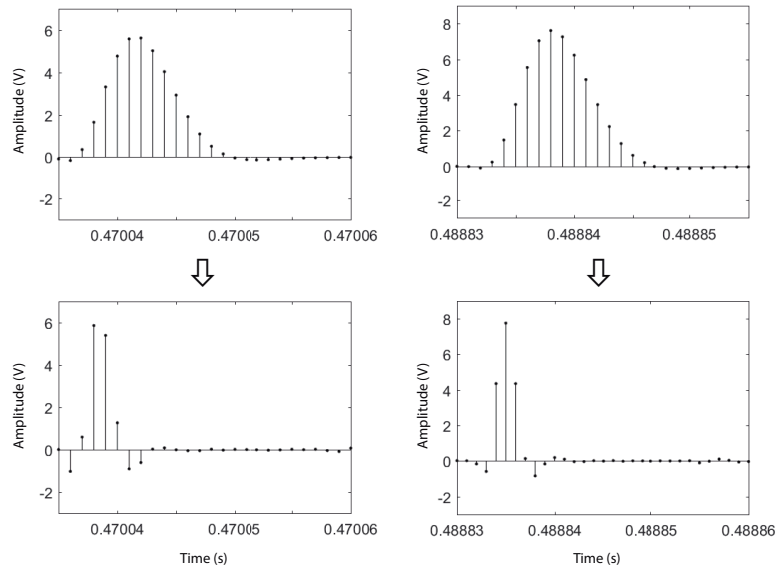


Figure 7: Example of unfolding of two pulses obtained from the Neutron Monitor. The signal amplitude is measured in volts at the output of the preamplifier.

125 the result of the unfolding, as well as their pole-zero diagrams, are shown in Fig. 8. The obtained results
 126 are similar to those obtained in [7].

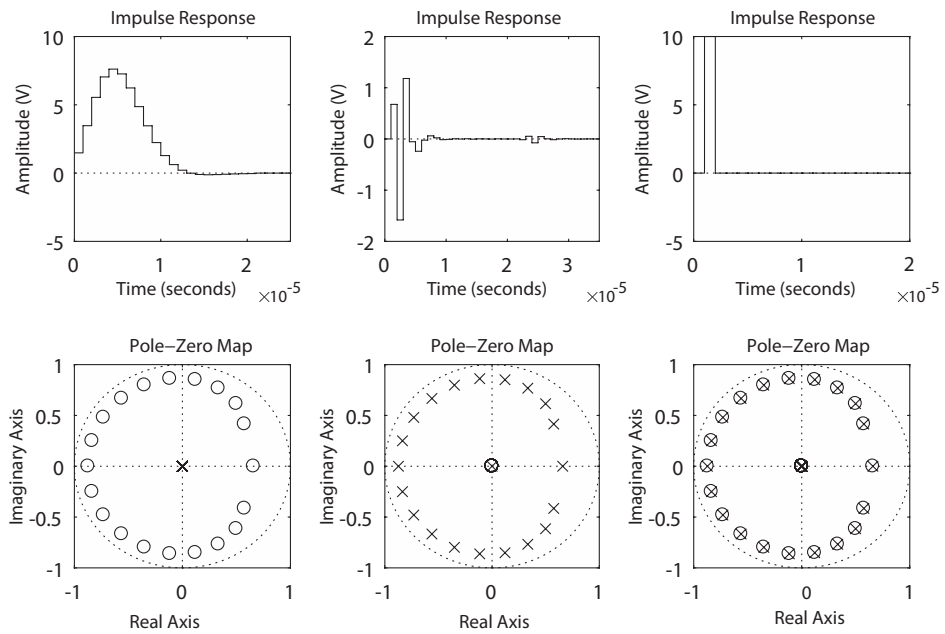


Figure 8: Unfolded signal (right) of an input signal (left) using the calculated unfolders (center).

127 The results for a non-delayed signal (i.e. $d = 0$) were identical to those of a delayed signal by one cycle,
 128 except that the unit impulse of the unfold and the unfolding (top-center and top-right graphs of Fig. 8)
 129 was advanced one cycle.

130 It should be noted that when the threshold level is very low, the unfold becomes unstable because a
 131 zero of the input signal turns up at $z = -3.3$ and therefore a pole of the unfold turns up at the same
 132 position. The effect is the same when the input signals starts slightly negative. This effect can be explained
 133 using Eq. (12). Dividing this equation between x_1 it results

$$\frac{h_i(z)}{x_1} = 1 + \frac{x_2}{x_1}z^{-1} + \frac{x_3}{x_1}z^{-2} + \dots + \frac{x_{21}}{x_1}z^{-20} \quad (13)$$

134 It is known from Vieta's Formulas that the second factor of a polynomial with a minus sign (in this case
 135 $-\frac{x_2}{x_1}$) is equal to the sum of all the roots of the polynomial. The smaller x_1 the larger the sum and so the
 136 roots (poles and zeros) will be closer to the limit of the ROC, even it may even exceed it. Nevertheless,
 137 raising the trigger makes the unfolded signal not an ideal unit impulse as seen in Fig. 8.

138 6. Conclusions

139 In this article, a method to determine when pulses coming from a radiation detector are unfoldable has
 140 been described and in such case, it allows to find the unfold characteristics and calculate its coefficients.
 141 Based on the properties of z-transform, we can conclude that whenever two pulses are unfoldable their sum
 142 and convolution are also unfoldable. Besides, their n-derivatives and n-integrals are unfoldable too. It is
 143 shown a set of examples of application of the method. Finally, it has been tested using pulses obtained from
 144 a radiation detector.

145 Acknowledgments

146 This project was funded by the Spanish Administration as part of the projects with ref. ESP2014-54505-
 147 C2 and ESP2015-68266-R.

148 References

- 149 [1] G. F. Knoll, Radiation Detection and Measurement, John Wiley & Sons, Inc., 2000.
- 150 [2] H. Spieler, Semiconductor Detector Systems, Oxford University Press, Oxford, 2005.
- 151 [3] F. S. Goulding, Nuclear Instruments and Methods 100 (1972) 493.
- 152 [4] M. Nakhostin, IEEE Transaction on Nuclear Science NS-58 (October(5)) (2011).
- 153 [5] V. T. Jordanov, Nuclear Instruments and Methods in Physics Research A 670 (2012) 18,
- 154 [6] J. Liu, et al., Nuclear Science and Techniques 28.7 (2017) 103.
- 155 [7] V. T. Jordanov, Nuclear Instruments and Methods in Physics Research A 805 (2016) 63.
- 156 [8] P. Fodisch, et al., Nuclear Instruments and Methods in Physics Research A 830 (2016) 484.

- 157 [9] R. W. Aldhaferi, International Journal of Electronics and Communications (AEÜ) 60 (2006) 413.
158 [10] A. Jazlan, et al., Australian Control Conference (AUCC) IEEE (2013) 79.
159 [11] J. Medina, et al., Nuclear Instruments and Methods in Physics Research A 727 (2013) 97.